enhAnced Mobile BiomEtRics

DELIVERABLE: D5.3

State of the Art Report ESR 4

Contract number:	675087
Project acronym:	AMBER
Project title:	Enhanced Mobile Biometrics
Project duration:	1 January 2017 – 31 December 2020
Coordinator:	Richard Guest, University of Kent, Canterbury, UK

Deliverable Number:	D39
Type:	R
Dissemination level	PU
Expected submission date	31.07.2019
Date submitted:	18.09.2019

Authors / contributors	Rıdvan Salih Kuzu, Patrizio Campisi
Contributing partners	UNIROMA3

This project has received funding from the European Union's Horizon 2020 research and innovation programme under the Marie Skłodowska-Curie grant agreement No 675087

On the cross-finger similarity of vein patterns

Emanuela Piciucco[0000−0001−7236−3511]
Ridvan Salih Kuzu[0000−0002−1816−181X]
Emanuele Maiorana[0000−0002−4312−6434]
Patrizio Campisi[0000−0002−1923−2739]

Roma Tre University, Via Vito Volterra 62, 00146 Rome, Italy[⋆]
{`emanuela.piciucco, ridvansalih.kuzu,`
`emanuele.maiorana, patrizio.campisi`}`@uniroma3.it`

Abstract. Biometric recognition based on finger-vein patterns is gaining more and more attention, as several approaches have been recently proposed to extract discriminative features from vascular structures. In this paper we investigate the similarity between vein patterns of symmetric fingers of the left and right hand of a subject. More in detail, we analyze the performance achievable when using symmetric fingers and geometry- or deep-learning-based feature extraction methods for recognition. A database with acquisitions from left and right index, medium, and ring fingers of 106 subjects is exploited for experimental tests.

Keywords: Biometrics, Finger-Vein Recognition, Convolutional Neural Networks

1 Introduction

Biometric systems are nowadays deployed in many practical applications requiring human recognition with high-level security, such as border controls, smartphone unlocking, ATM cash withdrawals, and e-commerce to cite a few. Among the exploitable biometric traits, vein patterns [9] have recently attracted a significant interest from industrial and academic communities, thanks to the several advantages they can offer with respect to other traditional biometric identifiers. In fact, the acquisition of vein patterns can be performed only in proximity through a near-infrared (NIR) camera, being therefore hard to implement presentation attacks. Moreover, being possible to perform a contactless recording of the interested train, vein-based biometric recognition systems ensure users' comfort and ease of use. Additionally, liveness detection is intrinsically provided.

Different kinds of vein patterns have been analyzed in literature for recognition purposes, namely finger veins [15], palm veins [22], hand dorsal veins and wrist veins [11]. For all the aforementioned traits, state-of-the-art approaches used for extracting representative features from the structure of blood vessels can be categorized into five classes:

- geometry-based [9, 10]: shape or topological structures are extracted from vein patterns and used as discriminative information. Most methods are based on the segmentation of the veins from the background, with features then extracted from the obtained patterns;

[⋆] This work has been supported by the EU Horizon 2020 Framework for Research and Innovation under Grant Agreement Number 675087 as part of the AMBER (enhAnced Mobile BiomEtRics) Marie Sklodowska-Curie project.

- statistical-based [13, 8]: statistical features, such as the local binary histogram and moments, are used to generate the employed templates;
- local invariant-feature-based [12]: algorithms such as scale invariant feature transform (SIFT) or speeded-up robust features (SURF) are employed to derive discriminative representations;
- subspace learning-based [17, 19]: methods such as linear discriminant analysis (LDA) or principal component analysis (PCA) are used to extract features;
- deep learning-based techniques [2, 3]: deep neural networks are exploited to learn discriminative representations from vein patterns. This latter approach has recently attracted a significant interest, being for instance used in [3], where two different light-weight CNNs have been examined for feature extraction from finger vein patterns. Generative adverserial networks (GANs) have been exploited for finger-vein-based biometric recognition in [20], while the Densenet-161 network has been applied to composite samples created from vein images in [16].

In this paper we focus on finger-vein biometric traits, and investigate the existence of similarities between vein patterns of symmetrical fingers belonging to left and right hands, in order to explicitly asses whether it could be possible, for recognition purposes, to consider pairs of symmetric fingers of a subjects as a single class. To the best of our knowledge, the aforementioned aspect has not been analyzed so far in literature for finger-vein-based biometric applications, while it has been evaluated when using palmprint [6, 18]. The research has highlighted the presence of shared patterns between the palmprints of both hands of a person, allowing a user to be recognized through his/her left palmprint even when only the other one has been recorded during enrolment. In order to perform a comprehensive analysis, the SDUMLA database [21], comprising finger-vein images from 106 users, with six samples for each of the left and right hand index, middle, and ring fingers, has been considered. Moreover, four different methods, belonging to the geometry- and deep-learning-based categories, have been exploited to derive the employed finger-vein feature representations.

2 Experimental Protocol

The purpose of the performed experimental tests is to verify whether finger-vein patterns of different hands of the same subject have a higher degree of similarity than traits belonging to different persons. To this aim, several tests have been performed on the SDUMLA databas, estimating the distributions of scores obtainable by comparing different classes of biometric samples, spcifically:

1. *genuine* scores are obtained by comparing vein patterns from the same finger of the same hand of the same subject. For instance, vein patterns of the right index of a subject are compared between themselves;
2. *impostor* scores are obtained by comparing veins from the same finger of the same hand of different subjects. For instance, patterns of the right index of a subject are compared with those of the right index of a different person;
3. *genuine cross-hand (CH)* scores are obtained by comparing veins from the same finger of different hands of the same subject. For instance, the right index of a subject is compared with the left index of the same person;

Table 1: Score distributions evaluated in the performed tests.

Case	**Subject**	**Hand**	**Finger**	**Scores**
1	same	same	same	genuine
2	different	same	same	impostor
3	same	different	same	genuine CH
4	same	same/different	different	genuine CF
5	different	same/different	different	impostor CF

4. *genuine cross-finger (CF)* scores are obtained by comparing veins from different fingers of the same subject. For instance, patterns of the right index are compared with those of the right/left middle finger of the same person;
5. *impostor cross-finger (CF)* scores are obtained by comparing veins from different fingers of different subjects. For instance, the right index of a subject is compared with the left/right middle finger of another person.

Table 1 summarizes the aforementioned combinations and the required scores. On the basis of the computed distributions, the false rejection rate (FRR) and the false acceptance rate (FAR) related to different scenarios have been evaluated:

1. *Test-1*: standard scenario where each finger from each hand is taken as a separate class, FRR and FAR are derived by considering respectively the aforementioned genuine scores and impostor scores;
2. *Test-2*: a naïve scenario where an impostor uses a finger different from the one enrolled by the legitimate user is taken into account. FRR and FAR respectively from genuine scores and impostor CF scores are evaluated;
3. *Test-3*: in order to verify whether a subject could be recognized by using as authentication probe the same finger of a hand different from the enrolled one, FRR and FAR are derived by considering respectively genuine scores and genuine CH scores;
4. *Test-4*: the feasibility of using interchangeably the same finger of different hands to be recognized is further investigated by evaluating the FRR and FAR computed respectively on genuine CH and impostor scores;
5. *Test-5*: eventually, the possibility of using as authentication probe fingers different from the enrolled one is also evaluated by deriving FRR and FAR respectively from genuine scores and genuine CF scores.

In order to obtain results from which reliable conclusions could be derived, the aforementioned score distributions have been computed according to several distinct processing methods described in the following section.

3 Finger-vein Recognition Methods

Score distributions have been computed by considering several different recognition methods, belonging to both geometry- and deep-learning-based approaches.

3.1 Geometry-based Finger-vein Recognition

Since the original vein images are typically characterized by low contrast, they are first enhanced in order to improve their quality using a contrast limited adaptive histogram equalization (CLAHE) [23]. Finger boundaries are then obtained by filtering the image with a mask [7]. Eventually, the finger is rotated and aligned to the image center as described in [4]. Finger vein patterns are extracted from finger areas using the following feature extraction methods:

1. *Maximum Curvature (MC)* [10]: scores related to veins width and curvature are assigned to positions where vein centers are located, which are then connected using filtering operations. Binary vein images are then obtained by thresholding the computed patterns;
2. *Principal Curvature (PC)* [1]: the image gradient field is computed, and noise components filtered out by means of hard thresholding. Values of principal curvature are first computed by considering the eigenvalue corresponding to the eigenvector of the Hessian matrix related to the maximum curvature, and then binarized to generate the desired template;
3. *Wide Line Detector (WLD)* [4]: vein positions are extracted by considering circular neighborhoods of each pixel, and computing differences between the center and its neighbors. The final binary image is determined by counting the number of pixels inside this neighborhood.

The obtained binary vein patterns are trimmed and then compared using the correlation-based method proposed in [9] and [10], with the maximum correlation used as matching score.

3.2 Deep-learning-based Finger-vein Recognition

Along with standard geometry-based recognition methods, tests have also been performed exploiting convolutional neural networks (CNNs) to obtain discriminative representations from finger-vein images. Since the target of the present study is not proposing a novel network architecture, an effective CNN, namely Densenet-201 [5], has been employed in the tests. Specifically, the final layers of a Densenet-201 architecture, that is, those performing classification after the extraction of discriminative features, have been substituted with:

- a batch-normalization layer, followed by a dropout regularization with 50% of hidden units dropped;
- a fully-connected and a batch-normalization layers producing C outputs, being C the number of unique identities considered for training.

Densenet's weights have been initialized with those estimated for an image classification task over Imagenet [14], while a unit weight initialization has been adopted for the batch normalization layer, and Glorot uniform initialization preferred for the fully-connected layers. The layers have been then updated using a cross-entropy (CE) loss function for back-propagation, with stochastic gradient descent (SGD) and a batch size of 64. Learning rate has been set to $\epsilon = 0.01$ and divided by 10 after each 30-epoch iteration. Momentum with $\alpha = 0.9$ has been used, as well as an L_2 weight decay regularization penalty with $\lambda = 0.025$. The maximum number of training epoch is set to 90, with early stopping in case the validation loss is minimized. In the testing phase, the features extracted by the employed network from two input finger-vein samples are compared by evaluating a cosine distance as score, to make geniune/impostor verification.

Table 2: EERs (in %) over the SDUMLA database for the performed tests.

Method	**Test-1**	**Test-2**	**Test-3**	**Test-4**	**Test-5**
MC	8.94	8.36	9.93	46.73	9.73
PC	11.70	11.07	12.81	46.64	12.95
WLD	13.66	12.72	14.50	45.56	14.66
CNN	1.02	0.54	1.73	32.62	1.69

4 Results and Discussion

The equal error rates (EERs) achieved with the considered recognition methods for each of the test conditions presented in Section 3 are reported in Table 2. It is worth mentioning that, since the standard approaches in Section 3.1 do not require any specific training, the associated performance has been computed considering all the available $106 \times 3 \times 2 = 636$ classes. Conversely, the results regarding the proposed CNN-based approach have been obtained while reserving the first half of the 106 subjects in the SDUMLA dataset for testing purposes, with the remaining 53 subjects used for CNN training. More in detail, two different training methodologies have been considered:

- to compute the scores associated with the distributions employed for Tests 1-3 and 5, the network has been trained with each finger of each hand of 53 subjects representing a different class. A total of $C = 53 \times 3 \times 2 = 318$ finger-vein classes have been therefore taken into account in this case. For each class, five out of the six available samples have been used for model training, with the remaining one employed for model validation;
- the scores of the distributions used for the considered Test 4, where the feasibility of using interchangeably the same finger of different hands to be recognized is analyzed, have been generated considered a network trained with the same fingers of different hands taken as the members of the same class. A total of $C = 53 \times 3 = 159$ classes have been therefore taken into account in this case. As left-right finger samples are put in the same category, each class is now represented with a total of 12 samples, 10 of which are fed into the model for training, while the remaining 2 samples are used for validation. Doing this, the network is trained to look for similarities between same fingers of different hands and associate them to the same class, thus allowing to evaluate the existence of such shared patterns.

The obtained results show that a pair of same fingers from different hands do not posses similarities that allow the user to be recognized when one finger is used for enrollement and the other one for recognition. This is evident by comparing the EERs achieved in Test-1 and Test-3, which are basically the same, meaning that scores generated by comparing same fingers from different hands of the same subject are similar to those obtained when comparing same fingers of different subjects. Actually, the former comparison seems to find some more similarities than the latter, as testified by the slightly worse EERs. Yet, such similarities cannot be assumed to be significant. Training a CNN while considering CH fingers as belonging to the same class further reinforce this considerations,

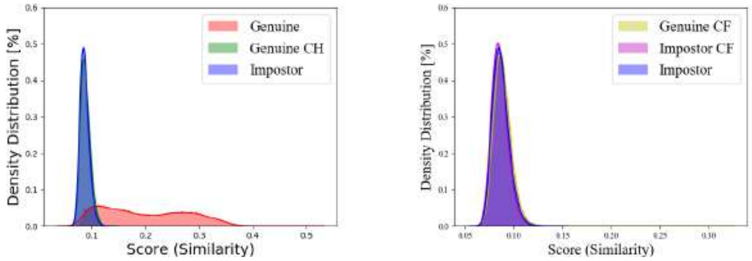

Fig. 1: Scores for the MC-based method. Left: genuine, impostor, and genuine CH distributions; Right: impostor, impostor CF, and genuine CF distributions.

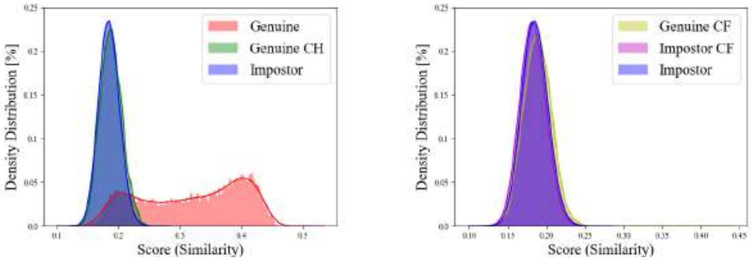

Fig. 2: Scores for the PC-based method. Left: genuine, impostor, and genuine CH distributions; Right: impostor, impostor CF, and genuine CF distributions.

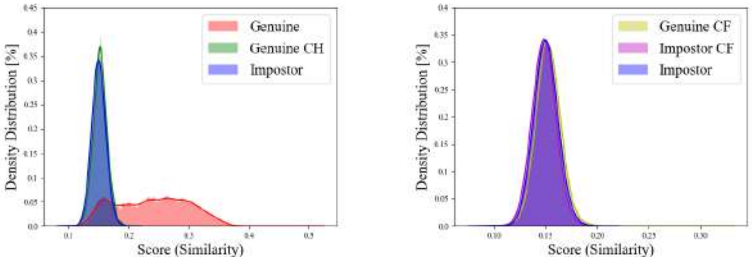

Fig. 3: Scores for the WLD-based method. Left: genuine, impostor, and genuine CH distributions; Right: impostor, impostor CF, and genuine CF distributions.

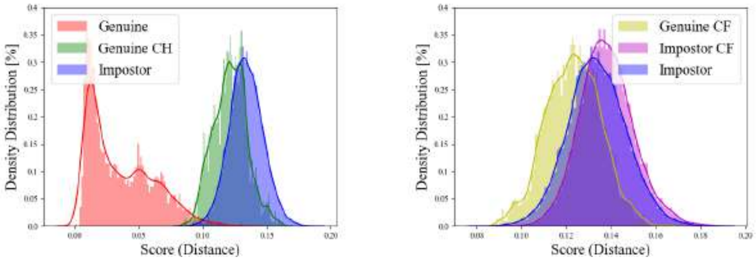

Fig. 4: Scores for the CNN-based method. Left: genuine, impostor, and genuine CH distributions; Right: impostor, impostor CF, and genuine CF distributions.

Table 3: Kullback-Leibler divergences with respect to genuine scores.

Method	impostor	genuine CH	genuine CF	impostor CF
MC	2.232	2.129	2.144	2.297
PC	1.877	1.761	1.747	1.956
WLD	1.718	1.658	1.633	1.790
CNN	0.237	0.106	0.058	0.281

as shown by the notably-high EER achieved in Test-4, which means the CNN cannot find shared patterns between pairs of fingers associated to the same class.

Interestingly, results in Test-5 also show that different fingers of the same subject share slightly more similarities than the same finger of different persons. Eventually, results in Test-2 suggest that the same fingers of different individuals are more similar than different fingers of different persons. Such resemblance may not necessarily spring from vein patterns, as it may depend on the geometric similarity of same fingers' shapes.

In order to provide further evidence of the observed behaviors, the computed score distributions are reported in Figures 1 - 4, where a training with 318 classes has been considered for the CNN-based approach. Genuine CH scores show basically the same distribution of impostor scores using geometry-based approaches, while resorting to CNNs highlights the existence of some similarities between pairs of symmetric fingers. CNNs are also able to generate slightly-different distributions for impostor, impostor CF and genuine CF scores, while geometry-based approaches cannot.

The distribution separations are quantitatively evaluated through the Kullback-Leibler divergences reported in Table 3, where the values obtained when evaluating the separation of impostor, impostor CF, genuine CH, and genuine CF distributions from that of genuine scores are considered. As can be seen, for CNNs genuine CH and genuine CF scores are slightly closer to the genuine ones than the impostors, while impostor CF scores are even farther.

5 Conclusions

A study regarding the similarity of the vein structure of symmetrical fingers of the hands for the purpose of biometric recognition has been conducted. The obtained results show that, although symmetrical fingers of the same subject show more resemblance than same fingers from different persons, such similarities are not significant enough to be exploited for recognition purposes.

References

1. Choi, J.H., Song, W., Kim, T., Lee, S.R., Kim, H.C.: Finger vein extraction using gradient normalization and principal curvature. In: SPIE Electronic Imaging (2009)
2. Das, R., Piciucco, E., Maiorana, E., Campisi, P.: Convolutional neural network for finger-vein-based biometric identification. IEEE Transactions on Information Forensics and Security **14**(2), 360–373 (2018)
3. Fang, Y., Wu, Q., Kang, W.: A novel finger vein verification system based on two-stream convolutional network learning. Neurocomputing **290**, 100–107 (2018)

4. Huang, B., Dai, Y., Li, R., Tang, D., Li, W.: Finger-vein authentication based on wide line detector and pattern normalization. In: Int. Conf. on Pattern Recognition (2010)
5. Huang, G., Liu, Z., Van Der Maaten, L., Weinberger, K.Q.: Densely connected convolutional networks. In: IEEE conference on computer vision and pattern recognition (2017)
6. Kumar, A., Wang, K.: Identifying humans by matching their left palmprint with right palmprint images using convolutional neural network. In: First Int. Workshop on Deep Learning and Pattern Recognition (2016)
7. Lee, E.C., Lee, H.C., Park, K.R.: Finger vein recognition using minutia-based alignment and local binary pattern-based feature extraction. Int. Journal of Imaging Systems and Technology **19**(3), 179–186 (2009)
8. Lee, E.C., Park, K.R.: Image restoration of skin scattering and optical blurring for finger vein recognition. Optics and Lasers in Engineering **49**(7), 816 – 828 (2011)
9. Miura, N., Nagasaka, A., Miyatake, T.: Feature extraction of finger vein patterns based on iterative line tracking and its application to personal identification. Systems and Computers in Japan **35**(7), 61–71 (2004)
10. Miura, N., Nagasaka, A., Miyatake, T.: Extraction of finger-vein patterns using maximum curvature points in image profiles. IEICE - Trans. Inf. Syst. **E90-D**(8), 1185–1194 (2007)
11. Pascual, J.E.S., Uriarte-Antonio, J., Sanchez-Reillo, R., Lorenz, M.G.: Capturing hand or wrist vein images for biometric authentication using low-cost devices. In: Int. Conf. on Intelligent Information Hiding and Multimedia Signal Processing (IIH-MSP) (2010)
12. Qin, H., Qin, L., Xue, L., He, X., Yu, C., Liang, X.: Finger-vein verification based on multi-features fusion. Sensors **13**(11), 15048–15067 (2013)
13. Rosdi, B.A., Shing, C.W., Suandi, S.A.: Finger vein recognition using local line binary pattern. Sensors **11**(12), 11357–11371 (2011)
14. Russakovsky, O., et al.: Imagenet large scale visual recognition challenge. International journal of computer vision **115**(3), 211–252 (2015)
15. Shaheed, K., Liu, H., Yang, G., Qureshi, I., Gou, J., Yin, Y.: A systematic review of finger vein recognition techniques. Information **9**(9), 213 (2018)
16. Song, J.M., Kim, W., Park, K.R.: Finger-Vein Recognition Based on Deep DenseNet Using Composite Image. IEEE Access (2019)
17. Wu, J.D., Liu, C.T.: Finger-vein pattern identification using principal component analysis and the neural network technique. Expert Systems with Applications **38**(5), 5423–5427 (2011)
18. Xu, Y., Fei, L., Zhang, D.: Combining left and right palmprint images for more accurate personal identification. IEEE transactions on image processing **24**(2), 549–559 (2014)
19. Yang, G., Xi, X., Yin, Y.: Finger vein recognition based on (2d) 2 pca and metric learning. BioMed Research Int. **2012** (2012)
20. Yang, W., Hui, C., Chen, Z., Xue, J.H., Liao, Q.: FV-GAN: Finger Vein Representation Using Generative Adversarial Networks. IEEE Transactions on Information Forensics and Security (2019)
21. Yin, Y., Liu, L., Sun, X.: SDUMLA-HMT: A Multimodal Biometric Database. Springer Berlin Heidelberg (2011)
22. Zhou, Y., Kumar, A.: Human identification using palm-vein images. IEEE Trans. on Information Forensics and Security **6**(4), 1259–1274 (Dec 2011)
23. Zuiderveld, K.: Contrast limited adaptive histogram equalization. In: Graphics gems IV (1994)